VIP Blood–Brain Barrier Very Important Paper

DOI: 10.1002/anie.201411226

A D-Peptide Ligand of Nicotine Acetylcholine Receptors for Brain-Targeted Drug Delivery**

Xiaoli Wei, Changyou Zhan, Qing Shen, Wei Fu, Cao Xie, Jie Gao, Chunmei Peng, Ping Zheng, and Weiyue Lu**

Abstract: *Lysosomes of brain capillary endothelial cells are implicated in nicotine acetylcholine receptor (nAChR)-mediated transcytosis and act as an enzymatic barrier for the transport of peptide ligands to the brain. A D-peptide ligand of nAChRs (termed ^{D}CDX), which binds to nAChRs with an IC_{50} value of 84.5 nM, was developed by retro–inverso isomerization. ^{D}CDX displayed exceptional stability in lysosomal homogenate and serum, and demonstrated significantly higher transcytosis efficiency in an in vitro blood–brain barrier monolayer compared with the parent L-peptide. When modified on liposomal surface, ^{D}CDX facilitated significant brain-targeted delivery of liposomes. As a result, brain-targeted delivery of ^{D}CDX modified liposomes enhanced therapeutic efficiency of encapsulated doxorubicin for glioblastoma. This study illustrates the importance of ligand stability in nAChRs-mediated transcytosis, and paves the way for developing stable brain-targeted entities.*

The blood-brain barrier (BBB), which mainly consists of the endothelial cells that line cerebral microvessels, prevents drugs and drug-delivery systems from reaching the site of central nervous system (CNS) diseases.[1] Receptor-mediated transcytosis (RMT) has been exploited as an efficient pathway to circumvent the BBB. Diverse receptors that expressed on brain capillary endothelial cells, including nicotine acetylcholine receptors (nAChRs),[2] transferrin receptors (TfR),[3] and low-density lipoprotein receptor-related protein-1 (LRP-1),[4] can recognize ligands in blood circulation and facilitate specific transport to the brain.

nAChRs are ligand-gated ion channels mainly expressed at neuromuscular junction of the CNS. Extensive expression of nAChRs on brain capillary endothelial cells and susceptibility to the inhibition by peptide neurotoxins and neurotropic viral proteins endow them with the ability to mediate peptide-based transvascular delivery of various therapeutic agents to the brain.[5] ^{L}CDX (FKESWREARGTRIERG), a 16-residue peptide developed by structure-guided design, demonstrates submicromolar binding affinity to nAChRs and enables micelle-based brain-targeted drug delivery.[6] To assess the trafficking route of ^{L}CDX upon nAChR-mediated transcytosis, intracellular distributions of endocytosed ^{L}CDX was investigated. Fluorescein-labeled ^{L}CDX was incubated with an in vitro BBB monolayer and intracellular fluorescence was detected 1 and 2 h after treatment. ^{L}CDX displayed punctuate intracellular distribution (Supporting Information, Figure S1), and the most of punctuate compartments colocalized with lysosome, suggesting the involvement of lysosome in nAChRs-mediated transcytosis. ^{L}CDX demonstrated high susceptibility to proteolytic degradation. The bulk of ^{L}CDX disappeared after 15 min incubation with lysosomal homogenate (Supporting Information, Figure S2), indicating that at least a part of endocytosed ^{L}CDX underwent intracellular degradation and the exocytosis was undermined.

We hypothesize that proteolytically stable ligands of nAChRs may possess higher brain targeting efficiency by overcoming the enzymatic barriers in brain capillary endothelial cells. ^{D}CDX, the retro–inverso isomer of ^{L}CDX, was chemically synthesized and its randomly coiled conformation was validated with circular dichroism spectrometry (Supporting Information, Figure S3). To investigate whether or not ^{D}CDX is capable of interacting with neuronal nAChRs, we conducted a competition binding assay where different concentrations of peptide competed for receptors binding with radiolabeled ^{125}I-α-bungarotoxin (^{125}I-α-Bgt), a natural antagonist of neuronal nAChRs. Both ^{D}CDX and ^{L}CDX functioned as competitive antagonists in a dose-dependent manner (Supporting Information, Figure S4). ^{D}CDX registered an IC_{50} value of 84.5 nM, which was approximately five times lower than that of ^{L}CDX (441.6 nM). To better understand the binding of ^{D}CDX to α7 neuronal nAChR, molecular modeling and docking were conducted on α7 nAChR with both ^{L}CDX and ^{D}CDX. The binding of both peptides to receptors was mainly dominated by electrostatic, cation–π, and hydrophobic interactions. ^{D}CDX underwent great conformational changes to enable the side chains to occupy the binding pocket of α7 nAChR (Supporting Information, Figure S6).

[*] X. Wei, Dr. C. Zhan, Q. Shen, Prof. W. Fu, C. Xie, J. Gao, C. Peng, Prof. W. Lu
Department of Pharmaceutics, School of Pharmacy
Fudan University & Key Laboratory of Smart Drug Delivery (Fudan University), Ministry of Education
Shanghai, 201203 (P.R. China)
E-mail: zcy439@hotmail.com
wylu@shmu.edu.cn
X. Wei, Prof. P. Zheng, Prof. W. Lu
State Key Laboratory of Medical Neurobiology
Fudan University, Shanghai, 200032 (P.R. China)
Prof. W. Lu
State Key Laboratory of Molecular Engineering of Polymers
Fudan University, Shanghai, 200433 (P.R. China)

[**] This work was supported by the National Basic Research Program of China (973 Program, 2013CB932500), National Natural Science Foundation of China (81273458 and 81473149), and National Science & Technology Major Project (2012ZX09304004).

Supporting information for this article is available on the WWW under http://dx.doi.org/10.1002/anie.201411226.

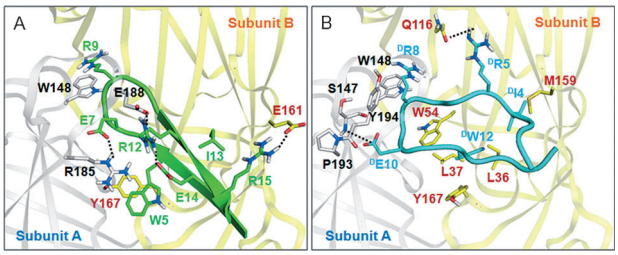

Figure 1. Binding mode of LCDX (A, green) and DCDX (B, aqua) with α7 nAChR. The subunit A of the receptor is shown in white and subunit B in yellow. Residues involved in binding are represented with sticks, and hydrogen bonds are denoted by black dashed lines.

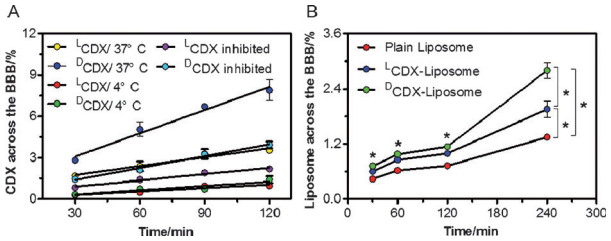

Figure 2. Transcytosis efficiency of DCDX, LCDX, and peptide-modified liposomes in the in vitro BBB monolayer. A) Fluorescein-labeled DCDX or LCDX (50 μM) was incubated at the luminal side of primary rat brain capillary endothelial cells monolayer at 4 °C and 37 °C, or with pre-incubation with 150 μM α-Bgt for one hour at 37 °C. At different time points, intact fluorescein labeled peptide at the abluminal side was analyzed by RP-HPLC coupled with a fluorescence detector (mean ± SD, $n = 3$). B) Transcytosis efficiency of DCDX-liposomes, LCDX-liposomes, and plain liposomes at 37 °C. Mean ± SD, $n = 3$, $^{*}p < 0.001$, DCDX-liposome vs. plain liposome at 30, 60, and 120 min.

Even though Arg9 in LCDX and its counterpart DArg8 in DCDX extended into the bottom of interfacial cleft and established a conserved cation–π interaction with Trp148[6,7] in subunit A, the two peptides displayed different binding modes (Figure 1; Supporting Information, S7–S9). Specifically, DGlu10 in DCDX inserted deeply into the binding pocket and formed hydrogen bond with NH group in the backbone of Ser147 and van der Waals interactions with the residues Pro193, Tyr194, Ser147, and Trp148 in subunit A, while the corresponding residue Glu7 in LCDX located outside the pocket and formed a hydrogen bond with Arg185 in subunit A. The side chain of DTrp12 in DCDX stretched deeply into the pocket and formed a hydrophobic interaction with Trp54, Leu36, and Leu37 in subunit B, while the counterpart Trp5 in LCDX interacted with Tyr167 in subunit B but did not bind into this hydrophobic pocket. The flexible character of DCDX made DArg5 form a hydrogen bond with Gln116 in subunit B, while the corresponding residue Arg12 in LCDX formed an intramolecular hydrogen bond with Glu14 in LCDX and a hydrogen bond with Glu188 in subunit A. The residue DIle4 in DCDX formed van der Waals interaction with the residue Met159 in subunit B, which was not found in the interactions of LCDX with α7 nAChR. However, Arg15 in LCDX formed a hydrogen bond with Glu161 in subunit B, which was not found in the interaction of DCDX with α7 nAChR. As a whole, DCDX displayed more potent interaction than did LCDX. Importantly, the binding affinities of the two peptides calculated for α7 nAChR by X-score were in good agreement with experimentally determined data (Supporting Information, Table S1), thus validating the design of DCDX as functional D-peptide antagonist of α7 nAChR.

To investigate the efficiency of nAChRs-mediated transcytosis, in vitro BBB monolayer was incubated with 50 μM fluorescein-labeled DCDX and LCDX at 37 °C. Solutions collected from the lower compartment at different time points were analyzed by reverse-phase HPLC coupled with a fluorescence detector. As shown in Figure 2 A, the percentage of DCDX across the BBB displayed a linear increase in a time-dependent fashion. After 2 h, 7.9 % DCDX traversed the in vitro BBB monolayer. However, LCDX displayed significantly lower efficiency at all tested time points in comparison to DCDX. When incubated at 4 °C, both peptides displayed minimum transcytosis efficiency over the BBB (< 1.0 %), which suggests energy consumption and possible participation of receptor mediation during transcytosis.[8] Considering that both DCDX and LCDX displayed high binding affinities to nAChRs, we studied potential participation of nAChRs during transcytosis. The BBB monolayer was pre-incubated with 150 μM α-Bgt for one hour to block nAChRs at the luminal side, followed by incubation with fluorescein labeled DCDX and LCDX. It was found that transcytosis of DCDX and LCDX was dramatically undermined with α-Bgt pretreatment, confirming that the transcytosis of DCDX and LCDX was mediated by nAChRs.

Liposome-based vehicle is a class of versatile nanocarriers for targeting delivery of various therapeutic agents.[9] Herein, we conjugated DCDX and LCDX on the surface of PEGylated liposomes to investigate the efficiency of nAChRs-mediated drug delivery to the brain. Rhodamine B-labeled liposomes were placed at the luminal side of in vitro BBB monolayer and fluorescence intensities at the abluminal side after different incubation periods were detected by fluorescence spectrophotometer. Liposomes were fluorescently labeled by inserting rhodamine B-conjugated 1,2-dipalmitoyl-sn-glycero-3-phosphoethanolamine (rhodamine B-DPPE), excluding the possibility that free dye was released from liposomes and crossed the in vitro BBB monolayer. As shown in Figure 2 B, DCDX and LCDX modification boosted liposome transcytosis. Among those, DCDX modification assumed the highest transcytosis efficiency of liposomes, which was consistent with the results of peptide transcytosis efficiency.

The intracellular distribution of the endocytosed DCDX in the in vitro BBB monolayer demonstrated the similar pathway to that of LCDX (Figure 3). Most of the peptide colocalized with lysosome. We also labeled early and late endosomes by using anti-EEA1 and anti-M6PR antibodies, respectively. Colocalization of CDX peptides with late endosome was evident and increased upon chase from 2 h to 12 h (Supporting Information, Figure S10). Both DCDX- and LCDX-liposomes exhibited obvious colocalization with lysosome of brain capillary endothelial cells (Figure S11), while plain liposomes displayed very low endocytosis efficiency (data not shown here). nAChRs-mediated endocytosis was previously revealed in C2C12 myocytes.[10] Binding of α-Bgt

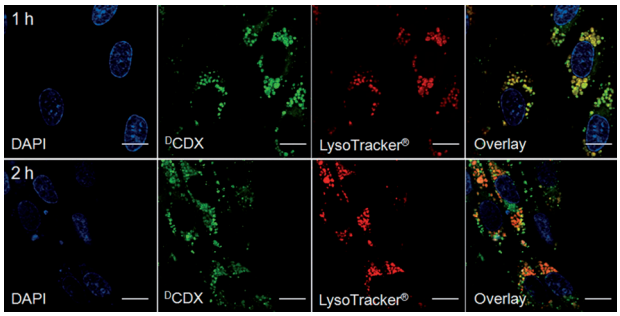

Figure 3. Colocalization of endocytosed DCDX and lysosome in the in vitro BBB monolayer. Fluorescein-labelled DCDX (50 μM) was incubated with in vitro BBB monolayer at 37 °C for 1 and 2 h, followed by lysosome staining. After fixation with formaldehyde, cells were subject to DAPI staining. Transwell membrane was detached and imaged by confocal laser scanning microscope. Scale bar = 10 μm.

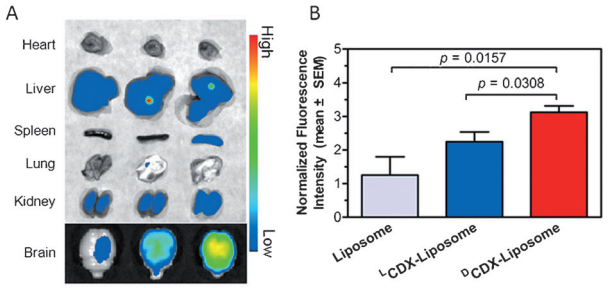

Figure 4. In vivo biodistribution of rhodamine B-labeled DCDX-liposomes, LCDX-liposomes, and plain liposomes. A) Ex vivo imaging of dissected tissues including brains and other organs of mice 8 h after injection. Organs from left to right are from mice administrated with plain liposomes, LCDX-liposomes, and DCDX-liposomes. B) Normalized fluorescence intensity of brain in each group. Mean ± SD, $n = 3$.

induces the internalization of cell surface nAChRs to late endosomes. This internalization occurs by sequestration of nAChR-α-Bgt complex in narrow, tubular, surface-connected compartments, while in the absence of clathrin, caveolin, or dynamin. However, the intracellular pathway of nAChRs-mediated transcytosis is unknown to date. Both DCDX and LCDX entered the brain capillary endothelial cells in the in vitro BBB monolayer and at least partially distributed in lysosomal compartments.

Different pathways have been proposed to depict the intracellular pathway of receptor-mediated transcytosis.[11] It is believed that lactoferrin[12] and low-density lipoprotein[13] bypass the lysosomal compartments by receptor mediation and are exocytosed without degradation; however, anti-TfR antibody (OX-26) was partially distributed in lysosome.[14] By virtue of exceptional stability of DCDX in lysosome homogenates, the participation of lysosomal compartments may at least partially explain the significantly higher transcytosis efficiency of DCDX displayed in the BBB model than that of LCDX. Lysosomal compartments may be quickly saturated with DCDX owing to full resistance of the D-peptide to proteolysis, resulting in higher efficiency of exocytotic transport than that of LCDX. In previous reports, lower-affinity antibody of TfR at therapeutic concentration (saturating concentration) demonstrated higher brain uptake capacity owing to the quick dissociation of antibody after receptor-mediated transcytosis than did higher-affinity antibody.[15] Herein, a high concentration of fluorescein-labeled peptides (50 μM) was incubated with the in vitro BBB monolayer to meet the detection limitation of analytic HPLC. The saturating concentration of peptides may lead to ligands binding to nAChRs on the luminal side of BBB regardless of affinities.

To study in vivo brain targeting efficiency, we compared brain distributions of DCDX and LCDX modified liposomes with plain liposomes. All of the liposomes were fluorescently labeled with rhodamine B-DPPE. Each labeled liposomal formulation was injected via a tail vein, and organs were harvested and subject to ex vivo fluorescent imaging 8 h after injection (Figure 4). It was evident that DCDX modification on the liposomal surface induced the highest brain distribution, validating high brain-targeting efficiency of DCDX in vivo. LCDX modification gave rise to higher fluorescence intensity in the brain in comparison to plain liposomes. The brains were sectioned and slices were examined with confocal laser scanning microscope for closer observation of in vivo liposome distribution (Supporting Information, Figure S12). DCDX-liposomes displayed higher distributions in cortex, hippocampus, and ventricle in comparison to LCDX-liposomes and plain liposomes.

To evaluate the potential therapeutic value of DCDX-decorated liposomes for CNS diseases, we studied the therapeutic efficacy of liposomal formulations encapsulating doxorubicin (DOX) in a xenograft nude mouse model of human glioblastoma multiforme (GBM). Five groups of nude mice ($n = 10$) bearing intracranial U87 cells were intravenously injected with saline, free DOX, DOX-loaded plain liposomes, DOX-loaded LCDX-liposomes, and DOX-loaded DCDX-liposomes. As shown in Figure 5, in the absence of CDX peptides, treatments with free or liposome-formulated doxorubicin at a dose of 2 mg per kg body weight (at 6, 9, 12, and 15 days post-tumor implantation) did little in improving mouse survival, registering a median survival of 26.5 days ($p = 0.105$) and 27 days ($p = 0.092$) versus 24 days for the saline-treated group. Both DCDX (33.5 days, $p < 0.005$) and LCDX

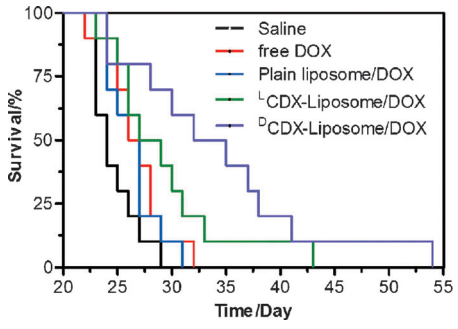

Figure 5. Kaplan–Meier survival curves of nude mice bearing intracranial U87 glioblastoma. Mice ($n = 10$) that received four doses (at 6, 9, 12, and 15 days after glioblastoma implantation) of DCDX (median survival time = 33.5 days) or LCDX-modified liposomes (median survival time = 28 days) encapsulating DOX survived significantly longer than the control groups that received saline (median survival time = 24 days).

(28 days, $p < 0.05$) decorating significantly prolonged the average survival time of nude mice. In comparison to plain liposomes containing DOX, ^{D}CDX modifiaction sigificantly lengthened the survival of model mice ($p < 0.005$). ^{D}CDX was superior to ^{L}CDX by extending additional 5.5 days (140% of the prolongation resulted from the treatment of ^{L}CDX-modified liposomes encapsulating DOX) of median survival time of intracranial GBM-bearing nude mice, in which BBB is the main obstacle to efficient drug delivery.[16]

Along with enzymatic barriers in brain capillary endothelial cells, blood plasma is another barrier to inactivate L-peptide ligand and undermine the interaction with nAChRs on the BBB. It was evident that ^{L}CDX demonstrated fast degradation and most intact peptide disappeared after 4 h incubation with 50% fresh rat serum. In conspicuous contrast, ^{D}CDX displayed nearly no degradation under the same condition (Figure 6). Preincubation with rat serum also

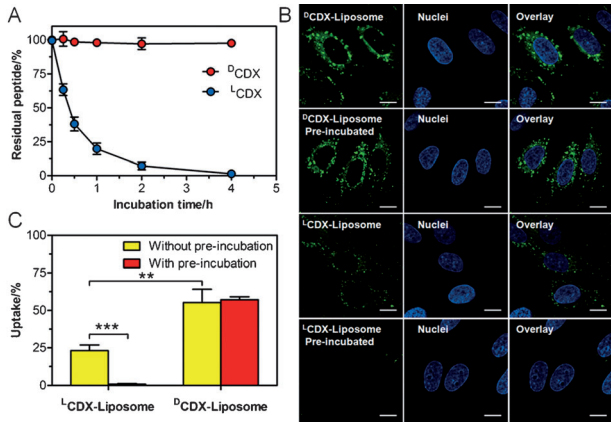

Figure 6. Stability of CDX peptides in 50% rat serum at 37°C and targeting ability of CDX peptides modified liposomes with brain capillary endothelial cells. A) Degradation of CDX peptide in 50% rat serum determined with HPLC. B) Brain capillary endothelial cells uptake of CDX peptides modified liposomes with and without pre-incubation with rat serum. C) Quantitative cellular uptake by using flow cytometer. Scale bar = 10 μm; $^{**}p < 0.005$, $^{***}p < 0.001$.

undermined the cellular uptake of ^{L}CDX-liposomes by brain capillary endothelial cells. Fluorescein loaded liposomes were incubated with cells for 4 h and intracellular fluorescence was tracked using confocal laser scanning microscope and flow cytometry. Both ^{D}CDX and ^{L}CDX modified liposomes were substantially taken up. After incubation with 50% rat serum, cellular uptake of pre-incubated ^{D}CDX modified liposomes exhibited no perceptible difference with that of non-treated ^{D}CDX-liposomes, whereas pre-incubation with rat serum significantly impaired the cellular uptake of ^{L}CDX-modified liposomes, indicating that D-peptide ligand modified liposomes are able to maintain fully targeting ability in blood circulation.

In the present study, a D-peptide ligand of nAChRs was developed to overcome enzymatic barriers in the BBB as well as in circulating blood. The function of ^{D}CDX as an antagonist of nAChRs was experimentally and computationally validated, and the brain targeting efficacy was evaluated in vitro and in vivo. When modified on the surface of PEGylated liposomes, ^{D}CDX efficiently inspired brain-targeted delivery of the encapsulated payloads. In vivo studies verified the potential value of ^{D}CDX in improving therapeutic efficacy of existing anticancer drugs such as doxorubicin in the treatment of glioblastoma. As the promising of D-peptide shown in brain-targeted drug delivery, the present study paved the way for designing proteolytically stable ligands of nAChRs for the treatment of CNS diseases.

Received: November 19, 2014
Published online: January 19, 2015

Keywords: blood–brain barrier · D-peptide ligands · glioblastoma · nicotine acetylcholine receptors

[1] a) W. M. Pardridge, *J. Cereb. Blood Flow Metab.* **2012**, *32*, 1959–1972; b) W. M. Pardridge, *Curr. Opin. Pharmacol.* **2006**, *6*, 494–500.
[2] a) P. Kumar, H. Wu, J. L. McBride, K. E. Jung, M. H. Kim, B. L. Davidson, S. K. Lee, P. Shankar, N. Manjunath, *Nature* **2007**, *448*, 39–43; b) S. Son, W. Hwang do, K. Singha, J. H. Jeong, T. G. Park, D. S. Lee, W. J. Kim, *J. Controlled Release* **2011**, *155*, 18–25; c) C. Zhan, Z. Yan, C. Xie, W. Lu, *Mol. Pharm.* **2010**, *7*, 1940–1947.
[3] a) W. M. Pardridge, J. L. Buciak, P. M. Friden, *J. Pharmacol. Exp. Ther.* **1991**, *259*, 66–70; b) P. M. Friden, *Neurosurgery* **1994**, *35*, 294–298; c) S. Skarlatos, T. Yoshikawa, W. M. Pardridge, *Brain Res.* **1995**, *683*, 164–171.
[4] a) H. Xin, X. Sha, X. Jiang, W. Zhang, L. Chen, X. Fang, *Biomaterials* **2012**, *33*, 8167–8176; b) M. Demeule, A. Regina, C. Che, J. Poirier, T. Nguyen, R. Gabathuler, J. P. Castaigne, R. Beliveau, *J. Pharmacol. Exp. Ther.* **2008**, *324*, 1064–1072; c) X. Wei, C. Zhan, X. Chen, J. Hou, C. Xie, W. Lu, *Mol. Pharm.* **2014**, *11*, 3261–3268.
[5] a) J. M. Lindstrom, *Ann. N. Y. Acad. Sci.* **2003**, *998*, 41–52; b) T. J. Abbruscato, S. P. Lopez, K. S. Mark, B. T. Hawkins, T. P. Davis, *J. Pharm. Sci.* **2002**, *91*, 2525–2538; c) C. Gotti, F. Clementi, *Prog. Neurobiol.* **2004**, *74*, 363–396; d) R. C. Hogg, M. Raggenbass, D. Bertrand, *Rev. Physiol. Biochem. Pharmacol.* **2003**, *147*, 1–46.
[6] C. Zhan, B. Li, L. Hu, X. Wei, L. Feng, W. Fu, W. Lu, *Angew. Chem. Int. Ed.* **2011**, *50*, 5482–5485; *Angew. Chem.* **2011**, *123*, 5596–5599.
[7] a) K. Brejc, W. J. van Dijk, R. V. Klaassen, M. Schuurmans, J. van Der Oost, A. B. Smit, T. K. Sixma, *Nature* **2001**, *411*, 269–276; b) Y. Bourne, T. T. Talley, S. B. Hansen, P. Taylor, P. Marchot, *EMBO J.* **2005**, *24*, 1512–1522; c) P. H. Celie, I. E. Kasheverov, D. Y. Mordvintsev, R. C. Hogg, P. van Nierop, R. van Elk, S. E. van Rossum-Fikkert, M. N. Zhmak, D. Bertrand, V. Tsetlin, T. K. Sixma, A. B. Smit, *Nat. Struct. Mol. Biol.* **2005**, *12*, 582–588.
[8] S. L. Schmid, L. L. Carter, *J. Cell Biol.* **1990**, *111*, 2307–2318.
[9] T. M. Allen, P. R. Cullis, *Science* **2004**, *303*, 1818–1822.
[10] S. Kumari, V. Borroni, A. Chaudhry, B. Chanda, R. Massol, S. Mayor, F. J. Barrantes, *J. Cell Biol.* **2008**, *181*, 1179–1193.
[11] U. Bickel, T. Yoshikawa, W. M. Pardridge, *Adv. Drug Delivery Rev.* **2001**, *46*, 247–279.
[12] C. Fillebeen, L. Descamps, M. P. Dehouck, L. Fenart, M. Benaissa, G. Spik, R. Cecchelli, A. Pierce, *J. Biol. Chem.* **1999**, *274*, 7011–7017.
[13] B. Dehouck, L. Fenart, M. P. Dehouck, A. Pierce, G. Torpier, R. Cecchelli, *J. Cell Biol.* **1997**, *138*, 877–889.

[14] E. Markoutsa, G. Pampalakis, A. Niarakis, I. A. Romero, B. Weksler, P. O. Couraud, S. G. Antimisiaris, *Eur. J. Pharm. Biopharm.* **2011**, *77*, 265 – 274.
[15] a) Y. J. Yu, Y. Zhang, M. Kenrick, K. Hoyte, W. Luk, Y. Lu, J. Atwal, J. M. Elliott, S. Prabhu, R. J. Watts, M. S. Dennis, *Sci. Transl. Med.* **2011**, *3*, 84ra44; b) Y. J. Yu, J. K. Atwal, Y. Zhang, R. K. Tong, K. R. Wildsmith, C. Tan, N. Bien-Ly, M. Hersom, J. A. Maloney, W. J. Meilandt, D. Bumbaca, K. Gadkar, K. Hoyte, W. Luk, Y. Lu, J. A. Ernst, K. Scearce-Levie, J. A. Couch, M. S. Dennis, R. J. Watts, *Sci. Transl. Med.* **2014**, *6*, 261ra154.
[16] a) C. Zhan, W. Lu, *Curr. Pharm. Biotechnol.* **2012**, *13*, 2380 – 2387; b) C. Zhan, Q. Meng, Q. Li, L. Feng, J. Zhu, W. Lu, *Chem. Asian J.* **2012**, *7*, 91 – 96.

